Modified projective synchronization with complex scaling factors of uncertain real chaos and complex chaos*

Zhang Fang-Fang(张芳芳)†, Liu Shu-Tang(刘树堂), and Yu Wei-Yong(余卫勇)

College of Control Science and Engineering, Shandong University, Jinan 250061, *China*

(Received 19 February 2013; revised manuscript received 23 April 2013)

To increase the variety and security of communication, we present the definitions of modified projective synchronization with complex scaling factors (CMPS) of real chaotic systems and complex chaotic systems, where complex scaling factors establish a link between real chaos and complex chaos. Considering all situations of unknown parameters and pseudo-gradient condition, we design adaptive CMPS schemes based on the speed-gradient method for the real drive chaotic system and complex response chaotic system and for the complex drive chaotic system and the real response chaotic system, respectively. The convergence factors and dynamical control strength are added to regulate the convergence speed and increase robustness. Numerical simulations verify the feasibility and effectiveness of the presented schemes.

Keywords: modified projective synchronization, complex scaling factors, complex chaotic systems, speed-gradient method

PACS: 05.45.Gg, 05.45.Xt, 05.45.Pq **DOI:** 10.1088/1674-1056/22/12/120505

1. Introduction

Since the seminal work by Pecora and Carrol,[1] chaos synchronization has been widely investigated for applications in secure communication.[2–5] Since Fowler *et al.*[6] introduced the complex Lorenz equations, the complex Chen and Lü systems have been proposed. These chaotic systems which involve complex variables are used to describe the physics of a detuned laser, rotating fluids, disk dynamos, electronic circuits, and particle beam dynamics in high energy accelerators. Now complex systems have played an important role in many branches of physics, e.g. fluids, superconductors, plasma physics, geophysical fluids, modulated optical waves, and electromagnetic fields.[7] The adoption of a complex chaotic system has also been proposed for secure communication, and the complex variables (doubling the number of variables) increase the contents and security of the transmitted information.[8] The idea is similar to the real chaotic system, i.e., chaotic signal is used as a carrier and transmitted together with an information signal to a receiver, and at the receiver end chaos synchronization is employed to recover the information signal.[9] Hence, the synchronization of complex chaotic systems has attracted greater attention in the last few decades, such as phase synchronization and anti-phase synchronization,[10] complete synchronization (CS),[11] anti-synchronization (AS),[12,13] lag synchronization (LS),[14] modified function projective synchronization(MFPS),[15] etc.

Recently, Hu *et al.*[16] observed hybrid projective synchronization (HPS), in which the different state variables can synchronize up to different scaling factors, in coupled partially linear chaotic complex nonlinear systems without adding any control term. Mahmoud and Mahmoud[17] investigated the phenomenon of projective synchronization (PS) and modified projective synchronization (MPS) of hyperchaotic attractors of hyperchaotic complex Lorenz system by active control. PS is a situation in which the state variables of the drive and response systems synchronize up to a real constant scaling factor δ (δ is a constant). MPS is defined if the responses of the synchronized dynamical states synchronize up to a real constant scaling matrix. Later, Liu Ping and Liu Shu-Tang[18] presented full state hybrid projective synchronization (FSHPS) with real scaling factors for two complex chaotic systems according to the definition of FSHPS for real chaotic systems.[19,20] In fact, the FSHPS is MPS of all state variables.

However, the above studies only touch on real scaling factors. In fact, the scaling factors can be complex for complex dynamical systems. The complex scaling factors establish a link between real chaotic systems and complex chaotic systems. If the drive system is real, we can adopt a complex system to synchronize the real drive system with complex scaling factors. It means that we obtain a complex signal from real chaotic signal multiplied by complex scaling factors, then the real part and the imaginary part of this complex signal are transmitted together with an information signal to a receiver, and at the receiver, we employ a complex system to synchronize to recover the information signal. Therefore, it is easy to transmit a complex signal. If the drive system is complex, we can adopt a real system to synchronize the real (imaginary) part of the product of complex drive system and complex scal-

*Project supported by the National Natural Science Foundation of China (Grant Nos. 61273088, 10971120, and 61001099) and the Natural Science Foundation of Shandong Province, China (Grant No. ZR2010FM010).

†Corresponding author. E-mail: zhff4u@163.com

© 2013 Chinese Physical Society and IOP Publishing Ltd

ing factors. It means the real (imaginary) part of this product is transmitted together with an information signal to a receiver, and at the receiver, we employ a real response system to synchronize this real (imaginary) part to recover the information signal. It will increase the range of choosing chaotic generators in the transmitters and receivers, thus an interceptor is harder to crack information sources.

In application to secure communications, Chee and Xu[21] extended binary digital to M-nary digital communication for achieving fast communication by manipulating the scaling feature of projective synchronization. The unpredictability of the scaling factor in projective synchronization can additionally enhance the security of communication. Since the complex scaling factors are arbitrary and more unpredictable than real scaling factors and the operations of complex numbers are complicated, the possibility that an interceptor extracts the information from the transmitted signal is greatly less than real scaling factors. Moreover, modified projective synchronization with complex scaling factors (CMPS) of real chaotic systems and complex chaotic systems will increase the complexity and scope of the synchronization, which will also increase security and variety of communications. Therefore, it is significant to study CMPS of real chaotic systems and complex chaotic systems. However, to the best of our knowledge, the CMPS has rarely been explored.

In practice, some systems' parameters cannot be exactly known, and the synchronization will be destroyed. For example, the receiver in secure communication is definitely suffering from all kinds of uncertainties such as uncertain parameters, which no doubt affects the precision of the communication. Therefore, we consider chaotic systems with unknown parameters. The adaptive control is one popular and useful approach to control and synchronize nonlinear chaotic systems with unknown parameters. Many researches[22–25] about the adaptive control of real uncertain chaotic systems are based on speed-gradient (SG) methodology. As for complex chaotic systems, Liu Shu-Tang and Liu Ping[12] preliminarily applied the SG method to the anti-synchronization of a class of uncertain chaotic complex systems; they also studied the FSHPS scheme with real scaling factors for a class of uncertain chaotic complex systems based on the SG method.[18] However, the adaption laws in these investigations do not contain convergence factors and pseudo-gradient conditions. Especially, they adopted the fixed control strength in error feedback wherever the initial points start, thus the strength must be maximal, which means a kind of waste in practice.[26] In a word, they did not indicate simple SG method clearly, and they did not consider convergence factors, pseudo-gradient condition, and the adaptive control strength. Besides, the number of unknown parameters in drive and response systems was the same, and either both were real or both were complex.

Inspired by the above discussion, we present CMPS of uncertain real chaotic systems and complex chaotic systems, considering all situations of unknown parameters based on the SG method with convergence factors, pseudo-gradient condition, and dynamical control strength.

The rest of the paper is organized as follows: the SG method is introduced in Section 2. We give the definition of CMPS of real drive chaotic system and complex response chaotic system and design the corresponding adaptive CMPS schemes in Section 3. In Section 4, we discuss the definition of CMPS of complex drive chaotic system and the real response chaotic system and corresponding CMPS schemes. In simulations, we realize CMPS of uncertain real hyperchaotic Rössler system and complex hyperchaotic Lorenz system and of complex Lorenz drive system and real Lorenz response system, respectively. Finally, some conclusions are given in Section 6.

2. Speed-gradient method

Consider the following n-dimensional real chaotic system

$$\dot{\boldsymbol{x}} = \boldsymbol{\phi}(\boldsymbol{x}, \theta, t), \tag{1}$$

where $\boldsymbol{x} = (x_1, x_2, \ldots, x_n)^{\mathrm{T}}$ is a real state vector (T denotes transpose), θ is a real matrix of unknown parameters. To output the desired signal $\boldsymbol{x}^*(t)$, we consider the error criterion function $\Phi(t) = \Phi(\boldsymbol{x}, t)$ (If $\boldsymbol{x}(t) \to \boldsymbol{x}^*(t), \Phi(\boldsymbol{x}, t) \to 0$) which is a scalar smooth nonnegative function. Its time derivative is

$$\omega(\theta, t) = \frac{\partial \Phi(\boldsymbol{x}, t)}{\partial t} + \nabla_{\boldsymbol{x}} \Phi(\boldsymbol{x}, t) \boldsymbol{\phi}(\boldsymbol{x}, \theta, t). \tag{2}$$

According to the speed-gradient method, the change of θ is along the opposite gradient direction of $\omega(\theta, t)$ in θ. The most general, i.e., the so-called combined form of the SG algorithm looks as follows:

$$\frac{\mathrm{d}}{\mathrm{d}t}(\theta + \varphi(t)) = -\Gamma \nabla_{\theta} \omega(\theta, t), \tag{3}$$

where Γ is a corresponding positive-definite gain matrix, and $\varphi(t)$ is a certain vector function satisfying the pseudogradient condition

$$\varphi^{\mathrm{T}}(t) \nabla_{\theta} \omega(\theta, t) \geq 0. \tag{4}$$

Equation (3) can also be written in the finite-integral form as

$$\theta = -\varphi(t) - \Gamma \int_0^t \nabla_{\theta} \omega(\theta, \alpha) \mathrm{d}\alpha. \tag{5}$$

The general stability theorem for combined SG law (3) is formulated below:

Lemma 1[22] Consider the systems (1) and (3) under the following assumptions:

Al) $\boldsymbol{\phi}(\boldsymbol{x}, \theta, t)$ and $\nabla_{\theta} \omega(\theta, t)$ are bounded together with their partial derivatives on any bounded set of states $(\boldsymbol{x}, \theta)$ of the systems (1) and (3) uniformly in $t \geq 0$ (regularity condition);

A2) $\omega(\theta,t)$ is convex in θ (convexity condition);

A3) There exist a real constant matrix θ^* and scalar uniformly continuous in each bounded region function $\rho(\boldsymbol{x}) \geq 0$, $\rho(0)=0$ such that inequality $\omega(\theta^*,t) \leq -\rho(\boldsymbol{x})$ holds for all $\boldsymbol{x} \in R^n$ (achievability condition);

A4) If $\Phi(\boldsymbol{x},t)$ is bounded then $\boldsymbol{x}(t)$ is bounded as well (boundedness condition);

Then each trajectory $(\boldsymbol{x}(t),\theta(t))$ of systems (1), (3), and (5) is bounded and $\lim_{t\to\infty}\rho(\boldsymbol{x}(t))=0$.

The proof is presented in the appendix of the literature[22] and thus is omitted.

3. CMPS schemes of real drive systems and complex response systems

3.1. Mathematical model and problem descriptions

Consider the following n-dimensional real drive chaotic system with unknown parameters,

$$\dot{\boldsymbol{z}} = \boldsymbol{G}(\boldsymbol{z})\boldsymbol{B} + \boldsymbol{g}(\boldsymbol{z}), \tag{6}$$

where $\boldsymbol{z} = (z_1, z_2, \ldots, z_n)^{\mathrm{T}}$ is a real state vector, $\boldsymbol{B} = (b_1, b_2, \ldots, b_s)^{\mathrm{T}}$ is an $s\times 1$ real vector of unknown parameters, and $\boldsymbol{G}(\boldsymbol{z})$ is an $n\times s$ real matrix, and $\boldsymbol{g} = (g_1, g_2, \ldots, g_n)^{\mathrm{T}}$ is a vector of real nonlinear function.

The complex response chaotic system is depicted as,

$$\dot{\boldsymbol{w}} = \boldsymbol{F}(\boldsymbol{w})\boldsymbol{A} + \boldsymbol{f}(\boldsymbol{w}) + \boldsymbol{v}, \tag{7}$$

where $\boldsymbol{w} = (w_1, w_2, \ldots, w_n)^{\mathrm{T}}$ is a complex state vector, and $\boldsymbol{w} = \boldsymbol{w}^{\mathrm{r}} + \mathrm{j}\boldsymbol{w}^{\mathrm{i}}$. Superscripts r and i stand for the real and imaginary parts of $\boldsymbol{w}$, respectively. Set $w_1 = u_1 + \mathrm{j}u_2$, $w_2 = u_3 + \mathrm{j}u_4, \ldots, w_n = u_{2n-1} + \mathrm{j}u_{2n}$, and $\boldsymbol{w}^{\mathrm{r}} = (u_1, u_3, \ldots, u_{2n-1})^{\mathrm{T}}$, $\boldsymbol{w}^{\mathrm{i}} = (u_2, u_4, \ldots, u_{2n})^{\mathrm{T}}$. $\boldsymbol{f} = (f_1, f_2, \ldots, f_n)^{\mathrm{T}}$ is a vector of complex nonlinear function, $\boldsymbol{F}(\boldsymbol{w})$ is an $n\times m$ complex matrix and its elements are functions of complex state variables, and $\boldsymbol{A} = (a_1, a_2, \ldots, a_m)^{\mathrm{T}}$ is an $m\times 1$ real (or complex) vector of unknown parameters. The designed controller is $\boldsymbol{v} = \boldsymbol{v}^{\mathrm{r}} + \mathrm{j}\boldsymbol{v}^{\mathrm{i}}$, where $\boldsymbol{v}^{\mathrm{r}} = (v_1, v_3, \ldots, v_{2n-1})^{\mathrm{T}}$, $\boldsymbol{v}^{\mathrm{i}} = (v_2, v_4, \ldots, v_{2n})^{\mathrm{T}}$.

According to the definition of MPS[17] and FSHPS[18] with real scaling factors of two chaotic complex systems, we give the definition of CMPS of real drive chaotic systems and complex response chaotic systems.

Definition 1 For the drive system (6) and response system (7), if there exists a complex constant matrix $\boldsymbol{H} = \mathrm{diag}\{h_1 + \mathrm{j}h_2, h_3 + \mathrm{j}h_4, \ldots, h_{2n-1} + \mathrm{j}h_{2n}\}$ such that

$$\begin{aligned}
&\lim_{t\to\infty}\|\boldsymbol{e}(t)\|^2 \\
&= \lim_{t\to\infty}\|\boldsymbol{w}(t) - \boldsymbol{H}\boldsymbol{z}(t)\|^2 \\
&= \lim_{t\to\infty}(\|\boldsymbol{w}(t)^{\mathrm{r}} - \boldsymbol{H}^{\mathrm{r}}\boldsymbol{z}(t)\|^2 + \|\boldsymbol{w}(t)^{\mathrm{i}} - \boldsymbol{H}^{\mathrm{i}}\boldsymbol{z}(t)\|^2) \\
&= 0,
\end{aligned} \tag{8}$$

where $\boldsymbol{e}(t)$ is the error vector, $\boldsymbol{e}^{\mathrm{r}}(t) = (e_1, e_3, \ldots, e_{2n-1})^{\mathrm{T}}$, $\boldsymbol{e}^{\mathrm{i}}(t) = (e_2, e_4, \ldots, e_{2n})^{\mathrm{T}}$, $\boldsymbol{H}^{\mathrm{r}} = \mathrm{diag}\{h_1, h_3, \ldots, h_{2n-1}\}$, $\boldsymbol{H}^{\mathrm{i}} = \mathrm{diag}\{h_2, h_4, \ldots, h_{2n}\}$, and $\|\cdot\|$ denotes the Euclidean norm of a vector, then the real drive system (6) and complex response system (7) are CMPS, and $h_1 + \mathrm{j}h_2, h_3 + \mathrm{j}h_4, \ldots, h_{2n-1} + \mathrm{j}h_{2n}$ are complex scaling factors. If there exists $w_l \in R$ $(l = 1, 2, \ldots, n)$, we select $h_{2l} = 0$ to avoid increasing a new imaginary part in the response system.

The control objective is to design an adaptive controller $\boldsymbol{v}$ such that the response complex system (7) can synchronize the drive real system (6) asymptotically in sense of the CMPS.

3.2. Adaptive CMPS schemes

If $\boldsymbol{A}$ is a real vector, according to the SG method, we have the following theorem.

Theorem 1 If the adaptive controller is designed as

$$\begin{aligned}
\boldsymbol{v} &= -\boldsymbol{F}(\boldsymbol{w})\hat{\boldsymbol{A}} - \boldsymbol{f}(\boldsymbol{w}) + \boldsymbol{H}\boldsymbol{G}(\boldsymbol{z})\hat{\boldsymbol{B}} + \boldsymbol{H}\boldsymbol{g}(\boldsymbol{z}) + \boldsymbol{K}\boldsymbol{e} \\
&= -\boldsymbol{F}(\boldsymbol{w})^{\mathrm{r}}\hat{\boldsymbol{A}} - \boldsymbol{f}(\boldsymbol{w})^{\mathrm{r}} + \boldsymbol{H}^{\mathrm{r}}\boldsymbol{G}(\boldsymbol{z})\hat{\boldsymbol{B}} + \boldsymbol{H}^{\mathrm{r}}\boldsymbol{g}(\boldsymbol{z}) + \boldsymbol{K}\boldsymbol{e}^{\mathrm{r}} \\
&\quad + [-\boldsymbol{F}(\boldsymbol{w})^{\mathrm{i}}\hat{\boldsymbol{A}} - \boldsymbol{f}(\boldsymbol{w})^{\mathrm{i}} + \boldsymbol{H}^{\mathrm{i}}\boldsymbol{G}(\boldsymbol{z})\hat{\boldsymbol{B}} \\
&\quad + \boldsymbol{H}^{\mathrm{i}}\boldsymbol{g}(\boldsymbol{z}) + \boldsymbol{K}\boldsymbol{e}^{\mathrm{i}}],
\end{aligned} \tag{9}$$

where $\boldsymbol{K} = \mathrm{diag}(k_1, k_2, \ldots, k_n)$ is the real control strength matrix and $\hat{\boldsymbol{A}}$, $\hat{\boldsymbol{B}}$ are the estimated values of $\boldsymbol{A}$ and $\boldsymbol{B}$, respectively; and the adaptive laws are selected as

$$\begin{cases}
\dot{\hat{\boldsymbol{A}}} = -\varphi_{\hat{\boldsymbol{A}}}(t) - \eta\int_0^t \nabla_{\hat{\boldsymbol{A}}}\omega(\hat{\boldsymbol{A}},\hat{\boldsymbol{B}},\alpha)\,\mathrm{d}\alpha, \\
\dot{\hat{\boldsymbol{B}}} = -\varphi_{\hat{\boldsymbol{B}}}(t) - \tau\int_0^t \nabla_{\hat{\boldsymbol{B}}}\omega(\hat{\boldsymbol{A}},\hat{\boldsymbol{B}},\alpha)\,\mathrm{d}\alpha, \\
\dot{k}_l = -\gamma_l[e_l^{\mathrm{r}}(t)^2 + e_l^{\mathrm{i}}(t)^2], \quad l = 1,2,\ldots,n,
\end{cases} \tag{10}$$

where

$$\nabla_{\hat{\boldsymbol{A}}}\omega(\hat{\boldsymbol{A}},\hat{\boldsymbol{B}},t) = -(\boldsymbol{F}^{\mathrm{T}}(\boldsymbol{w})^{\mathrm{r}}, \boldsymbol{F}^{\mathrm{T}}(\boldsymbol{w})^{\mathrm{i}})\begin{bmatrix}\boldsymbol{e}^{\mathrm{r}}\\ \boldsymbol{e}^{\mathrm{i}}\end{bmatrix}, \tag{11}$$

$$\nabla_{\hat{\boldsymbol{B}}}\omega(\hat{\boldsymbol{A}},\hat{\boldsymbol{B}},t) = ((\boldsymbol{H}^{\mathrm{r}}\boldsymbol{G}(\boldsymbol{z}))^{\mathrm{T}}, (\boldsymbol{H}^{\mathrm{i}}\boldsymbol{G}(\boldsymbol{z}))^{\mathrm{T}})\begin{bmatrix}\boldsymbol{e}^{\mathrm{r}}\\ \boldsymbol{e}^{\mathrm{i}}\end{bmatrix}, \tag{12}$$

and $\varphi_{\hat{\boldsymbol{A}}}(t) = \lambda\nabla_{\hat{\boldsymbol{A}}}\omega(\hat{\boldsymbol{A}},\hat{\boldsymbol{B}},t)$, $\varphi_{\hat{\boldsymbol{B}}}(t) = \varsigma\nabla_{\hat{\boldsymbol{B}}}\omega(\hat{\boldsymbol{A}},\hat{\boldsymbol{B}},t)$ which satisfy the pseudogradient condition, $\lambda = \mathrm{diag}(\lambda_1, \lambda_2, \ldots, \lambda_n)$, $\eta = \mathrm{diag}(\eta_1, \eta_2, \ldots, \eta_n)$, $\varsigma = \mathrm{diag}(\varsigma_1, \varsigma_2, \ldots, \varsigma_n)$, $\tau = \mathrm{diag}(\tau_1, \tau_2, \ldots, \tau_n)$, and $\gamma = \mathrm{diag}(\gamma_1, \gamma_2, \ldots, \gamma_n)$ are the corresponding convergence factor matrixes and their elements are positive real constants, then the complex response system (7) will synchronize the real drive system (6) in sense of CMPS asymptotically, and $\hat{\boldsymbol{A}}$, $\hat{\boldsymbol{B}}$ converge to constant vectors.

Proof From Eqs. (6), (7), and (9), we have

$$\begin{aligned}
\dot{\boldsymbol{e}} &= \dot{\boldsymbol{w}} - \dot{\boldsymbol{z}} \\
&= \boldsymbol{F}(\boldsymbol{w})\boldsymbol{A} + \boldsymbol{f}(\boldsymbol{w}) - \boldsymbol{F}(\boldsymbol{w})\hat{\boldsymbol{A}} - \boldsymbol{f}(\boldsymbol{w}) \\
&\quad + \boldsymbol{H}\boldsymbol{G}(\boldsymbol{z})\hat{\boldsymbol{B}} + \boldsymbol{H}\boldsymbol{g}(\boldsymbol{z}) + \boldsymbol{K}\boldsymbol{e} - \boldsymbol{H}\boldsymbol{G}(\boldsymbol{z})\boldsymbol{B} - \boldsymbol{H}\boldsymbol{g}(\boldsymbol{z}) \\
&= \boldsymbol{F}(\boldsymbol{w})(\boldsymbol{A} - \hat{\boldsymbol{A}}) - \boldsymbol{H}\boldsymbol{G}(\boldsymbol{z})(\boldsymbol{B} - \hat{\boldsymbol{B}}) + \boldsymbol{K}\boldsymbol{e} \\
&= \boldsymbol{F}(\boldsymbol{w})\tilde{\boldsymbol{A}} - \boldsymbol{H}\boldsymbol{G}(\boldsymbol{z})\tilde{\boldsymbol{B}} + \boldsymbol{K}\boldsymbol{e},
\end{aligned} \tag{13}$$

where $\tilde{\boldsymbol{A}} = \boldsymbol{A} - \hat{\boldsymbol{A}} = (\tilde{a}_1, \tilde{a}_2, \ldots, \tilde{a}_m)^{\mathrm{T}}$ and $\tilde{\boldsymbol{B}} = \boldsymbol{B} - \hat{\boldsymbol{B}} = (\tilde{b}_1, \tilde{b}_2, \ldots, \tilde{b}_s)^{\mathrm{T}}$ are the errors between the true values and estimated values of unknown parameters. Setting $\boldsymbol{\Psi}(\boldsymbol{z}) = \boldsymbol{HG}(\boldsymbol{z})$, we get $\boldsymbol{\Psi}(\boldsymbol{z})^{\mathrm{r}} = \boldsymbol{H}^{\mathrm{r}}\boldsymbol{G}(\boldsymbol{z})$, and $\boldsymbol{\Psi}(\boldsymbol{z})^{\mathrm{i}} = \boldsymbol{H}^{\mathrm{i}}\boldsymbol{G}(\boldsymbol{z})$. Therefore, we have $\dot{\boldsymbol{e}}^{\mathrm{r}} = \boldsymbol{F}(\boldsymbol{w})^{\mathrm{r}}\tilde{\boldsymbol{A}} - \boldsymbol{\Psi}(z)^{\mathrm{r}}\tilde{\boldsymbol{B}} + \boldsymbol{K}\boldsymbol{e}^{\mathrm{r}}$, $\dot{\boldsymbol{e}}^{\mathrm{i}} = \boldsymbol{F}(\boldsymbol{w})^{\mathrm{i}}\tilde{\boldsymbol{A}} - \boldsymbol{\Psi}(z)^{\mathrm{i}}\tilde{\boldsymbol{B}} + \boldsymbol{K}\boldsymbol{e}^{\mathrm{i}}$.

We introduce the following nonnegative Lyapunov function as

$$\begin{aligned} & V(e,t) \\ &= \frac{1}{2}[(\boldsymbol{e}^{\mathrm{r}})^{\mathrm{T}}\boldsymbol{e}^{\mathrm{r}} + (\boldsymbol{e}^{\mathrm{i}})^{\mathrm{T}}\boldsymbol{e}^{\mathrm{i}}] + \frac{1}{2}\eta^{-1}(\boldsymbol{A} - \hat{\boldsymbol{A}} - \varphi_{\hat{A}}(t))^2 \\ &\quad + \frac{1}{2}\tau^{-1}(\boldsymbol{B} - \hat{\boldsymbol{B}} - \varphi_{\hat{B}}(t))^2 + \frac{1}{2}\sum_{l=1}^{n}\frac{1}{\gamma_l}(k_l + L)^2, \end{aligned} \tag{14}$$

where L is an arbitrary large positive constant. From Eqs. (10)–(12), we have

$$\frac{\mathrm{d}}{\mathrm{d}t}(\tilde{\boldsymbol{A}} - \varphi_{\hat{\boldsymbol{A}}}(\boldsymbol{t})) = -\frac{\mathrm{d}}{\mathrm{d}t}(\hat{\boldsymbol{A}} + \varphi_{\hat{\boldsymbol{A}}}(\boldsymbol{t})) = \eta\nabla_{\hat{\boldsymbol{A}}}\omega(\hat{\boldsymbol{A}}, \hat{\boldsymbol{B}}, t)$$

and

$$\frac{\mathrm{d}}{\mathrm{d}t}(\tilde{\boldsymbol{B}} - \varphi_{\hat{\boldsymbol{B}}}(\boldsymbol{t})) = -\frac{\mathrm{d}}{\mathrm{d}t}(\hat{\boldsymbol{B}} + \varphi_{\hat{\boldsymbol{B}}}(\boldsymbol{t})) = \tau\nabla_{\hat{\boldsymbol{B}}}\omega(\hat{\boldsymbol{A}}, \hat{\boldsymbol{B}}, t),$$

then

$$\begin{aligned} \dot{V} &= (\dot{\boldsymbol{e}}^{\mathrm{r}})^{\mathrm{T}}\boldsymbol{e}^{\mathrm{r}} + (\dot{\boldsymbol{e}}^{\mathrm{i}})^{\mathrm{T}}\boldsymbol{e}^{\mathrm{i}} - \tilde{\boldsymbol{A}}[(F^{\mathrm{T}})^{\mathrm{r}}\boldsymbol{e}^{\mathrm{r}} + (F^{\mathrm{T}})^{\mathrm{i}}\boldsymbol{e}^{\mathrm{i}}] \\ &\quad - \lambda\nabla_{\hat{\boldsymbol{A}}}\omega(\hat{\boldsymbol{A}}, \hat{\boldsymbol{B}}, t)^2 + \tilde{\boldsymbol{B}}[(\boldsymbol{\Psi}^{\mathrm{T}})^{\mathrm{r}}\boldsymbol{e}^{\mathrm{r}} + (\boldsymbol{\Psi}^{\mathrm{T}})^{\mathrm{i}}\boldsymbol{e}^{\mathrm{i}}] \\ &\quad - \varsigma\nabla_{\hat{\boldsymbol{B}}}\omega(\hat{\boldsymbol{A}}, \hat{\boldsymbol{B}}, t)^2 - \sum_{l=1}^{n}(k_l + L)[e_l^{\mathrm{r}}(t)^2 + e_l^{\mathrm{i}}(t)^2] \\ &< (\boldsymbol{F}^{\mathrm{r}}\tilde{\boldsymbol{A}} - \boldsymbol{\Psi}^{\mathrm{r}}\tilde{\boldsymbol{B}} + \boldsymbol{K}\boldsymbol{e}^{\mathrm{r}})^{\mathrm{T}}\boldsymbol{e}^{\mathrm{r}} + (\boldsymbol{F}^{\mathrm{i}}\tilde{\boldsymbol{A}} - \boldsymbol{\Psi}^{\mathrm{i}}\tilde{\boldsymbol{B}} + \boldsymbol{K}\boldsymbol{e}^{\mathrm{i}})^{\mathrm{T}}\boldsymbol{e}^{\mathrm{i}} \\ &\quad - \tilde{\boldsymbol{A}}[(F^{\mathrm{T}})^{\mathrm{r}}\boldsymbol{e}^{\mathrm{r}} + (F^{\mathrm{T}})^{\mathrm{i}}\boldsymbol{e}^{\mathrm{i}}] + \tilde{\boldsymbol{B}}[(\boldsymbol{\Psi}^{\mathrm{T}})^{\mathrm{r}}\boldsymbol{e}^{\mathrm{r}} + (\boldsymbol{\Psi}^{\mathrm{T}})^{\mathrm{i}}\boldsymbol{e}^{\mathrm{i}}] \\ &\quad - \sum_{l=1}^{n}k_l[e_l^{\mathrm{r}}(t)^2 + e_l^{\mathrm{i}}(t)^2] - L\|\boldsymbol{e}\|^2 \\ &= -L\|\boldsymbol{e}\|^2. \end{aligned} \tag{15}$$

Conditions Al) and A2) are valid since the right-hand sides of Eqs. (9), (10), and (13) are smooth and linear in $\hat{\boldsymbol{A}}$ and $\hat{\boldsymbol{B}}$. Condition A3) is valid since for the constant matrixes $\boldsymbol{A}$ and $\boldsymbol{B}$ we have $\dot{V} < -L\|\boldsymbol{e}\|^2$, where $L\|\boldsymbol{e}\|^2 \geq 0$. The validity of condition A4) follows from the radial unboundedness of the objective function (14) and boundedness of the trajectories of the drive model (6). Since all conditions of Lemma 1 are satisfied we conclude that $\boldsymbol{w}(t)$, $\hat{\boldsymbol{A}}$, and $\hat{\boldsymbol{B}}$ are bounded, and $\lim_{t\to\infty}\|\boldsymbol{e}(\boldsymbol{t})\|^2 = 0$. We realize CMPS of system (6) and system (7). According to Eqs. (10)–(12), when $e(t) \to 0$, $\nabla_{\hat{\boldsymbol{A}}}\omega(\hat{\boldsymbol{A}}, \hat{\boldsymbol{B}}, t) \to 0$, and $\nabla_{\hat{\boldsymbol{B}}}\omega(\hat{\boldsymbol{A}}, \hat{\boldsymbol{B}}, t) \to 0$, therefore, $\hat{\boldsymbol{A}}$, $\hat{\boldsymbol{B}}$ converge to real constant vectors. The proof is completed.

If $\boldsymbol{A}$ is a complex vector, then $\boldsymbol{A}$ can be written as $\boldsymbol{A} = \boldsymbol{A}^{\mathrm{r}} + \mathrm{j}\boldsymbol{A}^{\mathrm{i}}$. Therefore, equation (7) becomes

$$\begin{aligned} \dot{\boldsymbol{w}} &= \boldsymbol{F}(\boldsymbol{w})\boldsymbol{A}^{\mathrm{r}} + \mathrm{j}\boldsymbol{F}(\boldsymbol{w})\boldsymbol{A}^{\mathrm{i}} + \boldsymbol{f}(\boldsymbol{w}) + \boldsymbol{v} \\ &= \boldsymbol{F}(\boldsymbol{w})\boldsymbol{A}^{\mathrm{r}} + \boldsymbol{R}(\boldsymbol{w})\boldsymbol{A}^{\mathrm{i}} + \boldsymbol{f}(\boldsymbol{w}) + \boldsymbol{v}, \end{aligned} \tag{16}$$

where $\boldsymbol{R}(\boldsymbol{w}) = \mathrm{j}\boldsymbol{F}(\boldsymbol{w})$ is a new $n \times m$ complex matrix. Therefore, we have

Theorem 2 If the adaptive controller is designed as

$$\begin{aligned} \boldsymbol{v} &= -\boldsymbol{F}(\boldsymbol{w})\hat{\boldsymbol{A}}^{\mathrm{r}} - \boldsymbol{R}(\boldsymbol{w})\hat{\boldsymbol{A}}^{\mathrm{i}} - \boldsymbol{f}(\boldsymbol{w}) + \boldsymbol{HG}(\boldsymbol{z})\hat{\boldsymbol{B}} \\ &\quad + \boldsymbol{Hg}(\boldsymbol{z}) + \boldsymbol{Ke} \\ &= -\boldsymbol{F}(\boldsymbol{w})^{\mathrm{r}}\hat{\boldsymbol{A}}^{\mathrm{r}} - \boldsymbol{R}(\boldsymbol{w})^{\mathrm{r}}\hat{\boldsymbol{A}}^{\mathrm{i}} - \boldsymbol{f}(\boldsymbol{w})^{\mathrm{r}} + \boldsymbol{H}^{\mathrm{r}}\boldsymbol{G}(\boldsymbol{z})\hat{\boldsymbol{B}} \\ &\quad + \boldsymbol{H}^{\mathrm{r}}\boldsymbol{g}(\boldsymbol{z}) + \boldsymbol{K}\boldsymbol{e}^{\mathrm{r}} + \mathrm{j}[-\boldsymbol{F}(\boldsymbol{w})^{\mathrm{i}}\hat{\boldsymbol{A}}^{\mathrm{r}} - \boldsymbol{R}(\boldsymbol{w})^{\mathrm{i}}\hat{\boldsymbol{A}}^{\mathrm{i}} \\ &\quad - \boldsymbol{f}(\boldsymbol{w})^{\mathrm{i}} + \boldsymbol{H}^{\mathrm{i}}\boldsymbol{G}(\boldsymbol{z})\hat{\boldsymbol{B}} + \boldsymbol{H}^{\mathrm{i}}\boldsymbol{g}(\boldsymbol{z}) + \boldsymbol{K}\boldsymbol{e}^{\mathrm{i}}], \end{aligned} \tag{17}$$

and the adaptive laws are selected as

$$\begin{cases} \dot{\hat{\boldsymbol{A}}}^{\mathrm{r}} = -\lambda\nabla_{\hat{\boldsymbol{A}}^{\mathrm{r}}}\omega(\hat{\boldsymbol{A}}^{\mathrm{r}}, \hat{\boldsymbol{A}}^{\mathrm{i}}, \hat{\boldsymbol{B}}, t) \\ \qquad\quad -\eta\int_0^t\nabla_{\hat{\boldsymbol{A}}^{\mathrm{r}}}\omega(\hat{\boldsymbol{A}}^{\mathrm{r}}, \hat{\boldsymbol{A}}^{\mathrm{i}}, \hat{\boldsymbol{B}}, \alpha)\mathrm{d}\alpha, \\ \dot{\hat{\boldsymbol{A}}}^{\mathrm{i}} = -\lambda'\nabla_{\hat{\boldsymbol{A}}^{\mathrm{i}}}\omega(\hat{\boldsymbol{A}}^{\mathrm{r}}, \hat{\boldsymbol{A}}^{\mathrm{i}}, \hat{\boldsymbol{B}}, t) \\ \qquad\quad -\eta'\int_0^t\nabla_{\hat{\boldsymbol{A}}^{\mathrm{i}}}\omega(\hat{\boldsymbol{A}}^{\mathrm{r}}, \hat{\boldsymbol{A}}^{\mathrm{i}}, \hat{\boldsymbol{B}}, \alpha)\mathrm{d}\alpha, \\ \dot{\hat{\boldsymbol{B}}} = -\varsigma\nabla_{\hat{\boldsymbol{B}}}\omega(\hat{\boldsymbol{A}}^{\mathrm{r}}, \hat{\boldsymbol{A}}^{\mathrm{i}}, \hat{\boldsymbol{B}}, t) \\ \qquad\quad -\tau\int_0^t\nabla_{\hat{\boldsymbol{B}}}\omega(\hat{\boldsymbol{A}}^{\mathrm{r}}, \hat{\boldsymbol{A}}^{\mathrm{i}}, \hat{\boldsymbol{B}}, \alpha)\mathrm{d}\alpha, \\ \dot{k}_l = -\gamma_l[e_l^{\mathrm{r}}(t)^2 + e_l^{\mathrm{i}}(t)^2], \quad l = 1, 2, \ldots, n, \end{cases} \tag{18}$$

where

$$\begin{aligned} & \nabla_{\hat{\boldsymbol{A}}^{\mathrm{r}}}\omega(\hat{\boldsymbol{A}}^{\mathrm{r}}, \hat{\boldsymbol{A}}^{\mathrm{i}}, \hat{\boldsymbol{B}}, t) \\ &= -(\boldsymbol{F}^{\mathrm{T}}(\boldsymbol{w})^{\mathrm{r}}, \boldsymbol{F}^{\mathrm{T}}(\boldsymbol{w})^{\mathrm{i}})\begin{bmatrix}\boldsymbol{e}^{\mathrm{r}} \\ \boldsymbol{e}^{\mathrm{i}}\end{bmatrix}, \end{aligned} \tag{19}$$

$$\begin{aligned} & \nabla_{\hat{\boldsymbol{A}}^{\mathrm{i}}}\omega(\hat{\boldsymbol{A}}^{\mathrm{r}}, \hat{\boldsymbol{A}}^{\mathrm{i}}, \hat{\boldsymbol{B}}, t) \\ &= -(\boldsymbol{R}^{\mathrm{T}}(\boldsymbol{w})^{\mathrm{r}}, \boldsymbol{R}^{\mathrm{T}}(\boldsymbol{w})^{\mathrm{i}})\begin{bmatrix}\boldsymbol{e}^{\mathrm{r}} \\ \boldsymbol{e}^{\mathrm{i}}\end{bmatrix}, \end{aligned} \tag{20}$$

$$\begin{aligned} & \nabla_{\hat{\boldsymbol{B}}}\omega(\hat{\boldsymbol{A}}^{\mathrm{r}}, \hat{\boldsymbol{A}}^{\mathrm{i}}, \hat{\boldsymbol{B}}, t) \\ &= ((\boldsymbol{H}^{\mathrm{r}}\boldsymbol{G}(\boldsymbol{z}))^{\mathrm{T}}, (\boldsymbol{H}^{\mathrm{i}}\boldsymbol{G}(\boldsymbol{z}))^{\mathrm{T}})\begin{bmatrix}\boldsymbol{e}^{\mathrm{r}} \\ \boldsymbol{e}^{\mathrm{i}}\end{bmatrix}, \end{aligned} \tag{21}$$

where $\lambda' = \mathrm{diag}(\lambda_1', \lambda_2', \ldots, \lambda_n')$ and $\eta' = \mathrm{diag}(\eta_1', \eta_2', \ldots, \eta_n')$ are corresponding convergence factor matrixes and their elements are positive real constants, then the response system (16) synchronizes the real drive chaotic system (6) in sense of CMPS asymptotically, and $\hat{\boldsymbol{A}}^{\mathrm{r}}$, $\hat{\boldsymbol{A}}^{\mathrm{i}}$, $\hat{\boldsymbol{B}}$ converge to real constant vectors.

Proof It is similar to the proof in Theorem 1 and thus is omitted.

4. CMPS schemes of complex drive chaotic system and real response chaotic system

4.1. Mathematical model and problem descriptions

In this section, we consider the following n-dimensional complex drive chaotic system with unknown parameters,

$$\dot{\boldsymbol{y}} = \boldsymbol{Q}(\boldsymbol{y})\boldsymbol{D} + \boldsymbol{q}(\boldsymbol{y}), \tag{22}$$

where $\boldsymbol{y} = (y_1, y_2, \ldots, y_n)^{\mathrm{T}}$ is a complex state vector. Set $y_1 = u_1' + \mathrm{j}u_2'$, $y_2 = u_3' + \mathrm{j}u_4'$, $\ldots$, $y_n = u_{2n-1}' + \mathrm{j}u_{2n}'$, and $\boldsymbol{y}^{\mathrm{r}} =$

$(u'_1, u'_3, \ldots, u'_{2n-1})^{\mathrm{T}}$, $\boldsymbol{y}^{\mathrm{i}} = (u'_2, u'_4, \ldots, u'_{2n})^{\mathrm{T}}$. $\boldsymbol{Q}(y)$ is an $n \times s$ complex matrix and its elements are functions of complex state variables, $\boldsymbol{D} = (d_1, d_2, \ldots, d_s)^{\mathrm{T}}$ is an $s \times 1$ real (complex) vector of unknown parameters, and $\boldsymbol{q} = (q_1, q_2, \ldots, q_n)^{\mathrm{T}}$ is a vector of a complex nonlinear function.

The real response chaotic system is depicted as,

$$\dot{\boldsymbol{x}} = \boldsymbol{P}(\boldsymbol{x})\boldsymbol{C} + \boldsymbol{p}(\boldsymbol{x}) + \boldsymbol{L}, \tag{23}$$

where $\boldsymbol{x} = (x_1, x_2, \ldots, x_n)^{\mathrm{T}}$ is a real state vector. $\boldsymbol{P}(\boldsymbol{x})$ is an $n \times m$ real matrix, and $\boldsymbol{C} = (c_1, c_2, \ldots, c_m)^{\mathrm{T}}$ is an $m \times 1$ real vector of unknown parameters, and $\boldsymbol{p} = (p_1, p_2, \ldots, p_n)^{\mathrm{T}}$ is a vector of real nonlinear function. The designed controller is $\boldsymbol{L}$.

We first give the special definition of CMPS of complex drive chaotic systems and real response chaotic systems.

Definition 2 For the drive system (22) and response system (23), if there exists a complex constant matrix $\boldsymbol{H} = \mathrm{diag}\{h_1 + \mathrm{j}h_2, h_3 + \mathrm{j}h_4, \ldots, h_{2n-1} + \mathrm{j}h_{2n}\}$ such that

$$\lim_{t\to\infty} \|\boldsymbol{e}(t)\|^2 = \lim_{t\to\infty} \|\boldsymbol{x}(t) - \boldsymbol{H}^{\mathrm{r}}\boldsymbol{y}^{\mathrm{r}}(t) + \boldsymbol{H}^{\mathrm{i}}\boldsymbol{y}^{\mathrm{i}}(t)\|^2 = 0, \tag{24}$$

where $\boldsymbol{e}(t) = \boldsymbol{x}(t) - \boldsymbol{H}^{\mathrm{r}}\boldsymbol{y}^{\mathrm{r}}(t) + \boldsymbol{H}^{\mathrm{i}}\boldsymbol{y}^{\mathrm{i}}(t)$ is the real error vector, then the complex drive system (22) and real response system (23) are CMPS of real parts. As $\boldsymbol{x}(t)$ is real, we choose real $\boldsymbol{L}$ to ensure CMPS of real parts and avoid increasing the imaginary parts of response system. The control objective is to design an adaptive real controller $\boldsymbol{L}$ such that the response real system (23) can synchronize the drive complex system (22) asymptotically in sense of the CMPS of real parts.

4.2. Adaptive CMPS schemes of real parts

If $\boldsymbol{D}$ is a real vector, we have the following theorem.

Theorem 3 If the adaptive controller is designed as

$$\begin{aligned}\boldsymbol{L} = {} & -\boldsymbol{P}(\boldsymbol{x})\hat{\boldsymbol{C}} - \boldsymbol{p}(\boldsymbol{x}) + (\boldsymbol{H}^{\mathrm{r}}\boldsymbol{Q}(\boldsymbol{y})^{\mathrm{r}} - \boldsymbol{H}^{\mathrm{i}}\boldsymbol{Q}(\boldsymbol{y})^{\mathrm{i}})\hat{\boldsymbol{D}} \\ & + \boldsymbol{H}^{\mathrm{r}}\boldsymbol{q}(\boldsymbol{y})^{\mathrm{r}} - \boldsymbol{H}^{\mathrm{i}}\boldsymbol{q}(\boldsymbol{y})^{\mathrm{i}} + \boldsymbol{K}\boldsymbol{e},\end{aligned} \tag{25}$$

where $\hat{\boldsymbol{C}}$, $\hat{\boldsymbol{D}}$ are the estimated values of $\boldsymbol{C}$ and $\boldsymbol{D}$, respectively; and the adaptive laws are selected as

$$\begin{cases} \dot{\hat{\boldsymbol{C}}} = -\lambda\nabla_{\hat{\boldsymbol{C}}}\omega(\hat{\boldsymbol{C}}, \hat{\boldsymbol{D}}, t) - \eta\int_0^t \nabla_{\hat{\boldsymbol{C}}}\omega(\hat{\boldsymbol{C}}, \hat{\boldsymbol{D}}, \alpha)\,\mathrm{d}\alpha, \\ \dot{\hat{\boldsymbol{D}}} = -\varsigma\nabla_{\hat{\boldsymbol{D}}}\omega(\hat{\boldsymbol{C}}, \hat{\boldsymbol{D}}, t) - \tau\int_0^t \nabla_{\hat{\boldsymbol{D}}}\omega(\hat{\boldsymbol{C}}, \hat{\boldsymbol{D}}, \alpha)\,\mathrm{d}\alpha, \\ \dot{k}_l = -\gamma_l[e_l^{\mathrm{r}}(t)^2 + e_l^{\mathrm{i}}(t)^2], \quad l = 1, 2, \cdots, n, \end{cases} \tag{26}$$

where

$$\nabla_{\hat{\boldsymbol{C}}}\omega(\hat{\boldsymbol{C}}, \hat{\boldsymbol{D}}, t) = -\boldsymbol{P}^{\mathrm{T}}(\boldsymbol{x})\boldsymbol{e}, \tag{27}$$

$$\nabla_{\hat{\boldsymbol{D}}}\omega(\hat{\boldsymbol{C}}, \hat{\boldsymbol{D}}, t) = (\boldsymbol{H}^{\mathrm{r}}\boldsymbol{Q}(\boldsymbol{y})^{\mathrm{r}} - \boldsymbol{H}^{\mathrm{i}}\boldsymbol{Q}(\boldsymbol{y})^{\mathrm{i}})^{\mathrm{T}}\boldsymbol{e}, \tag{28}$$

then the response system (23) and the drive chaotic system (22) will be CMPS for real parts and $\hat{\boldsymbol{C}}$, $\hat{\boldsymbol{D}}$ converge to real constant vectors.

Proof It is similar to the proof in Theorem 1 and thus is omitted.

If $\boldsymbol{D}$ is a complex vector, then $\boldsymbol{D}$ can be written as $\boldsymbol{D} = \boldsymbol{D}^{\mathrm{r}} + \mathrm{j}\boldsymbol{D}^{\mathrm{i}}$ and expression (22) becomes

$$\begin{aligned}\dot{\boldsymbol{y}} &= \boldsymbol{Q}(\boldsymbol{y})\boldsymbol{D}^{\mathrm{r}} + \mathrm{j}\boldsymbol{Q}(\boldsymbol{y})\boldsymbol{D}^{\mathrm{i}} + \boldsymbol{q}(\boldsymbol{y}) \\ &= \boldsymbol{Q}(\boldsymbol{y})\boldsymbol{D}^{\mathrm{r}} + \boldsymbol{O}(\boldsymbol{y})\boldsymbol{D}^{\mathrm{i}} + \boldsymbol{q}(\boldsymbol{y}),\end{aligned} \tag{29}$$

where $\boldsymbol{O}(\boldsymbol{y}) = \mathrm{j}\boldsymbol{Q}(\boldsymbol{y})$ is a new $n \times m$ complex matrix. Therefore, we have the following theorem.

Theorem 4 If the adaptive controller is designed as

$$\begin{aligned}\boldsymbol{L} = {} & -\boldsymbol{P}(\boldsymbol{x})\hat{\boldsymbol{C}} - \boldsymbol{p}(\boldsymbol{x}) + (\boldsymbol{H}^{\mathrm{r}}\boldsymbol{Q}(\boldsymbol{y})^{\mathrm{r}} - \boldsymbol{H}^{\mathrm{i}}\boldsymbol{Q}(\boldsymbol{y})^{\mathrm{i}})\hat{\boldsymbol{D}}^{\mathrm{r}} \\ & + (\boldsymbol{H}^{\mathrm{r}}\boldsymbol{O}(\boldsymbol{y})^{\mathrm{r}} - \boldsymbol{H}^{\mathrm{i}}\boldsymbol{O}(\boldsymbol{y})^{\mathrm{i}})\hat{\boldsymbol{D}}^{\mathrm{i}} + \boldsymbol{H}^{\mathrm{r}}\boldsymbol{q}(\boldsymbol{y})^{\mathrm{r}} \\ & - \boldsymbol{H}^{\mathrm{i}}\boldsymbol{q}(\boldsymbol{y})^{\mathrm{i}} + \boldsymbol{K}\boldsymbol{e}\end{aligned} \tag{30}$$

and the adaptive laws are selected as

$$\begin{cases} \dot{\hat{\boldsymbol{C}}} = -\lambda\nabla_{\hat{\boldsymbol{C}}}\omega(\hat{\boldsymbol{C}}, \hat{\boldsymbol{D}}^{\mathrm{r}}, \hat{\boldsymbol{D}}^{\mathrm{i}}, t) \\ \qquad\quad - \eta\int_0^t \nabla_{\hat{\boldsymbol{C}}}\omega(\hat{\boldsymbol{C}}, \hat{\boldsymbol{D}}^{\mathrm{r}}, \hat{\boldsymbol{D}}^{\mathrm{i}}, \alpha)\,\mathrm{d}\alpha, \\ \dot{\hat{\boldsymbol{D}}}^{\mathrm{r}} = -\varsigma\nabla_{\hat{\boldsymbol{D}}^{\mathrm{r}}}\omega(\hat{\boldsymbol{C}}, \hat{\boldsymbol{D}}^{\mathrm{r}}, \hat{\boldsymbol{D}}^{\mathrm{i}}, t) \\ \qquad\quad - \tau\int_0^t \nabla_{\hat{\boldsymbol{D}}^{\mathrm{r}}}\omega(\hat{\boldsymbol{C}}, \hat{\boldsymbol{D}}^{\mathrm{r}}, \hat{\boldsymbol{D}}^{\mathrm{i}}, \alpha)\,\mathrm{d}\alpha, \\ \dot{\hat{\boldsymbol{D}}}^{\mathrm{i}} = -\varsigma'\nabla_{\hat{\boldsymbol{D}}^{\mathrm{i}}}\omega(\hat{\boldsymbol{C}}, \hat{\boldsymbol{D}}^{\mathrm{r}}, \hat{\boldsymbol{D}}^{\mathrm{i}}, t) \\ \qquad\quad - \tau'\int_0^t \nabla_{\hat{\boldsymbol{D}}^{\mathrm{i}}}\omega(\hat{\boldsymbol{C}}, \hat{\boldsymbol{D}}^{\mathrm{r}}, \hat{\boldsymbol{D}}^{\mathrm{i}}, \alpha)\,\mathrm{d}\alpha, \\ \dot{k}_l = -\gamma_l[e_l^{\mathrm{r}}(t)^2 + e_l^{\mathrm{i}}(t)^2], \quad l = 1, 2, \ldots, n, \end{cases} \tag{31}$$

where

$$\nabla_{\hat{\boldsymbol{C}}}\omega(\hat{\boldsymbol{C}}, \hat{\boldsymbol{D}}^{\mathrm{r}}, \hat{\boldsymbol{D}}^{\mathrm{i}}, t) = -\boldsymbol{P}^{\mathrm{T}}(\boldsymbol{x})\boldsymbol{e}, \tag{32}$$

$$\nabla_{\hat{\boldsymbol{D}}^{\mathrm{r}}}\omega(\hat{\boldsymbol{C}}, \hat{\boldsymbol{D}}^{\mathrm{r}}, \hat{\boldsymbol{D}}^{\mathrm{i}}, t) = (\boldsymbol{H}^{\mathrm{r}}\boldsymbol{Q}(\boldsymbol{y})^{\mathrm{r}} - \boldsymbol{H}^{\mathrm{i}}\boldsymbol{Q}(\boldsymbol{y})^{\mathrm{i}})^{\mathrm{T}}\boldsymbol{e}, \tag{33}$$

$$\nabla_{\hat{\boldsymbol{D}}^{\mathrm{i}}}\omega(\hat{\boldsymbol{C}}, \hat{\boldsymbol{D}}^{\mathrm{r}}, \hat{\boldsymbol{D}}^{\mathrm{i}}, t) = (\boldsymbol{H}^{\mathrm{r}}\boldsymbol{O}(\boldsymbol{y})^{\mathrm{r}} - \boldsymbol{H}^{\mathrm{i}}\boldsymbol{O}(\boldsymbol{y})^{\mathrm{i}})^{\mathrm{T}}\boldsymbol{e}, \tag{34}$$

where $\varsigma' = \mathrm{diag}(\varsigma'_1, \varsigma'_2, \ldots, \varsigma'_n)$ and $\tau' = \mathrm{diag}(\tau'_1, \tau'_2, \ldots, \tau'_n)$ are the convergence factor matrix and its elements are positive real constants, then the response system (23) and the drive chaotic system (29) will be CMPS for real parts, and $\hat{\boldsymbol{C}}$, $\hat{\boldsymbol{D}}^{\mathrm{r}}$, $\hat{\boldsymbol{D}}^{\mathrm{i}}$ converge to real constant vectors.

Proof It is similar to the proof in Theorem 1 and thus is omitted.

Obviously, the CMPS of imaginary parts is similar to the CMPS of real parts, and thus is omitted.

5. Simulations

5.1. CMPS of real hyperchaotic Rössler system and complex hyperchaotic Lorenz system

In order to observe CMPS behaviors of the real drive system and complex response system, we assume that the real hyperchaotic Rössler system[27] drives the complex hyperchaotic Lorenz system.[28] The drive hyperchaotic Rössler system is defined as follows:

$$\begin{cases} \dot{z}_1 = -z_2 - z_3, \\ \dot{z}_2 = z_1 + b_1 z_2 + z_4, \\ \dot{z}_3 = b_2 + z_1 z_3, \\ \dot{z}_4 = -b_3 z_3 + b_4 z_4, \end{cases} \tag{35}$$

where

$$\boldsymbol{G}(\boldsymbol{z}) = \begin{pmatrix} 0 & 0 & 0 & 0 \\ z_2 & 0 & 0 & 0 \\ 0 & 1 & 0 & 0 \\ 0 & 0 & -z_3 & z_4 \end{pmatrix}, \quad \boldsymbol{g}(\boldsymbol{z}) = \begin{pmatrix} -z_2 - z_3 \\ z_1 + z_4 \\ z_1 z_3 \\ 0 \end{pmatrix},$$

and z_1, z_2, z_3, and z_4 are real state variables, $\boldsymbol{B} = (b_1, b_2, b_3, b_4)^{\mathrm{T}}$ is the unknown parameter vector.

The complex response hyperchaotic Lorenz system is

$$\begin{cases} \dot{w}_1 = a_1(w_2 - w_1), \\ \dot{w}_2 = a_2 w_1 - w_2 - w_1 w_3 + w_4, \\ \dot{w}_3 = -a_3 w_3 + (1/2)(\bar{w}_1 w_2 + w_1 \bar{w}_2), \\ \dot{w}_4 = a_4 w_1 + a_5 w_2, \end{cases} \tag{36}$$

where

$$\boldsymbol{F}(\boldsymbol{w}) = \begin{pmatrix} w_2 - w_1 & 0 & 0 & 0 & 0 \\ 0 & w_1 & 0 & 0 & 0 \\ 0 & 0 & -w_3 & 0 & 0 \\ 0 & 0 & 0 & w_1 & w_2 \end{pmatrix},$$

$$\boldsymbol{f}(\boldsymbol{w}) = \begin{pmatrix} 0 \\ -w_2 - w_1 w_3 + w_4 \\ (1/2)(\bar{w}_1 w_2 + w_1 \bar{w}_2) \\ 0 \end{pmatrix},$$

where $w_1 = u_1 + \mathrm{j}u_2$, $w_2 = u_3 + \mathrm{j}u_4$, $w_4 = u_6 + \mathrm{j}u_7$ are complex state variables and $w_3 = u_5$ is a real state variable, a_1, a_2, a_3, a_4, a_5 are real unknown parameters. The overbar $\bar{w}_1(\bar{w}_2)$ stands for the complex conjugate of $w_1(w_2)$.

We design the controller according to Theorem 1 as follows:

$$\begin{aligned} \boldsymbol{v} &= -\boldsymbol{F}(\boldsymbol{w})\hat{\boldsymbol{A}} - \boldsymbol{f}(\boldsymbol{w}) + \boldsymbol{H}\boldsymbol{G}(\boldsymbol{z})\hat{\boldsymbol{B}} + \boldsymbol{H}\boldsymbol{g}(\boldsymbol{z}) + \boldsymbol{K}\boldsymbol{e} \\ &= \begin{pmatrix} -\hat{a}_1(w_2 - w_1) + (h_1 + \mathrm{j}h_2)(-z_2 - z_3) + k_1(e_1 + \mathrm{j}e_2) \\ -\hat{a}_2 w_1 + w_2 + w_1 w_3 - w_4 + (h_3 + \mathrm{j}h_4)(z_1 + \hat{b}_1 z_2 + z_4) + k_2(e_3 + \mathrm{j}e_4) \\ \hat{a}_3 w_3 - (1/2)(\bar{w}_1 w_2 + w_1 \bar{w}_2) + h_5(\hat{b}_2 + z_1 z_3) + k_3 e_5 \\ -\hat{a}_4 w_1 - \hat{a}_5 w_2 + (h_6 + \mathrm{j}h_7)(-\hat{b}_3 z_3 + \hat{b}_4 z_4) + k_4(e_6 + \mathrm{j}e_7) \end{pmatrix} \\ &= \begin{pmatrix} -\hat{a}_1(u_3 - u_1) + h_1(-z_2 - z_3) + k_1 e_1 \\ -\hat{a}_2 u_1 + u_3 + u_1 u_5 - u_6 + h_3(z_1 + \hat{b}_1 z_2 + z_4) + k_2 e_3 \\ \hat{a}_3 u_5 - (u_1 u_3 + u_2 u_4) + h_5(\hat{b}_2 + z_1 z_3) + k_3 e_5 \\ -\hat{a}_4 u_1 - \hat{a}_5 u_3 + h_6(-\hat{b}_3 z_3 + \hat{b}_4 z_4) + k_4 e_6 \end{pmatrix} + \mathrm{j} \begin{pmatrix} -\hat{a}_1(u_4 - u_2) + h_2(-z_2 - z_3) + k_1 e_2 \\ -\hat{a}_2 u_2 + u_4 + u_2 u_5 - u_7 + h_4(z_1 + \hat{b}_1 z_2 + z_4) + k_2 e_4 \\ 0 \\ -\hat{a}_4 u_2 - \hat{a}_5 u_4 + h_7(-\hat{b}_3 z_3 + \hat{b}_4 z_4) + k_4 e_7 \end{pmatrix}, \end{aligned} \tag{37}$$

where $h_1 + \mathrm{j}h_2$, $h_3 + \mathrm{j}h_4$, h_5, $h_6 + \mathrm{j}h_7$ are scaling factors, $e_1 = u_1 - h_1 z_1$, $e_2 = u_2 - h_2 z_1$, $e_3 = u_3 - h_3 z_2$, $e_4 = u_4 - h_4 z_2$, $e_5 = u_5 - h_5 z_3$, $e_6 = u_6 - h_6 z_4$, and $e_7 = u_7 - h_7 z_4$.

The adaptive laws are taken as Eq. (10), where

$$\nabla_{\hat{\boldsymbol{A}}}\omega(\hat{\boldsymbol{A}}, \hat{\boldsymbol{B}}, t) = \begin{pmatrix} -[(u_3 - u_1)e_1 + (u_4 - u_2)e_2] \\ -[u_1 e_3 + u_2 e_4] \\ u_5 e_5 \\ -(u_1 e_6 + u_2 e_7) \\ -(u_3 e_6 + u_4 e_7) \end{pmatrix}, \tag{38}$$

$$\nabla_{\hat{\boldsymbol{B}}}\omega(\hat{\boldsymbol{A}}, \hat{\boldsymbol{B}}, t) = \begin{pmatrix} h_3 z_2 e_3 + h_4 z_2 e_4 \\ h_5 e_5 \\ -h_6 z_3 e_6 - h_7 z_3 e_7 \\ h_6 z_4 e_6 + h_7 z_4 e_7 \end{pmatrix}, \tag{39}$$

and

$$\dot{\boldsymbol{k}} = \begin{pmatrix} \dot{k}_1 \\ \dot{k}_2 \\ \dot{k}_3 \\ \dot{k}_4 \end{pmatrix} = \begin{pmatrix} -\gamma_1(e_1^2 + e_2^2) \\ -\gamma_2(e_3^2 + e_4^2) \\ -\gamma_3 e_5^2 \\ -\gamma_4(e_6^2 + e_7^2) \end{pmatrix}. \tag{40}$$

The true values of unknown parameters are $\boldsymbol{A} = (14, 35, 3, -5, -4)^{\mathrm{T}}$ and $\boldsymbol{B} = (0.25, 3, 0.5, 0.05)^{\mathrm{T}}$. The initial conditions of the drive system (35) and the response system (36) are $\boldsymbol{z}(\boldsymbol{0}) = (-20, 0, 0, 15)^{\mathrm{T}}$ and $\boldsymbol{w}(\boldsymbol{0}) = (-1 - 2\mathrm{j}, -3 - 4\mathrm{j}, -5, -6 - 7\mathrm{j})^{\mathrm{T}}$. The initial values of estimated parameters and control strength are $\hat{\boldsymbol{A}}(0) = (10, 10, 10, 10, 10)^{\mathrm{T}}$, $\hat{\boldsymbol{B}}(0) = (1, 1, 1, 1)^{\mathrm{T}}$, and $\boldsymbol{k}(0) = (0, 0, 0, 0)^{\mathrm{T}}$. The fourth-order Runge–Kutta scheme is utilized to solve the differential equations with $\Delta t = 10^{-3}$ s. The CMPS process of systems (35) and (36) is shown in Fig. 1, where the solid line shows the states of the drive system and the dotted line presents the states of the response system. Their chaotic behaviors are shown in Figs. 2 and 3, where the red line shows the trajectory of the drive system and the blue line presents the trajectory of the response system. The real parts $(w_1^{\mathrm{r}}, w_2^{\mathrm{r}}, w_3)$ of the response system (36) completely synchronize (z_1, z_2, z_3) of the drive system (35) in Fig. 2 as $h_1 = h_3 = h_5 = 1$, while the imaginary parts $(w_1^{\mathrm{i}}, w_2^{\mathrm{i}}, w_4^{\mathrm{i}})$ of the response system (36) anti-synchronize (z_1, z_2, z_4) of the drive system (35) in Fig. 3 as $h_2 = h_4 = h_7 = -1$. The errors of CMPS converge asymptotically to zero as demonstrated in Fig. 4.

The processes of parameters identification of $\hat{\boldsymbol{A}}$ and $\hat{\boldsymbol{B}}$ are shown in Figs. 5 and 6 respectively. The estimated vector $\hat{\boldsymbol{A}}$ converges to

$$(14.0383, 34.9475, 2.9451, -5.0000, -4.0000)^{\mathrm{T}}$$

while $\hat{\boldsymbol{B}}$ converges to $(0.2071, 3.0332, 0.5231, 0.0523)^{\mathrm{T}}$, which are near the true value.

5.2. CMPS of complex Lorenz drive system and real Lorenz response system

In order to observe CMPS behaviors of the complex drive system and the real response system, we assume that the uncertain complex Lorenz system drives the uncertain real Lorenz system. Therefore, the complex drive system is defined as follows:

$$\begin{cases} \dot{y}_1 = d_1(y_2 - y_1), \\ \dot{y}_2 = d_2 y_1 - y_1 y_3 - y_2, \\ \dot{y}_3 = -d_3 y_3 + (1/2)(\bar{y}_1 y_2 + y_1 \bar{y}_2), \end{cases} \tag{41}$$

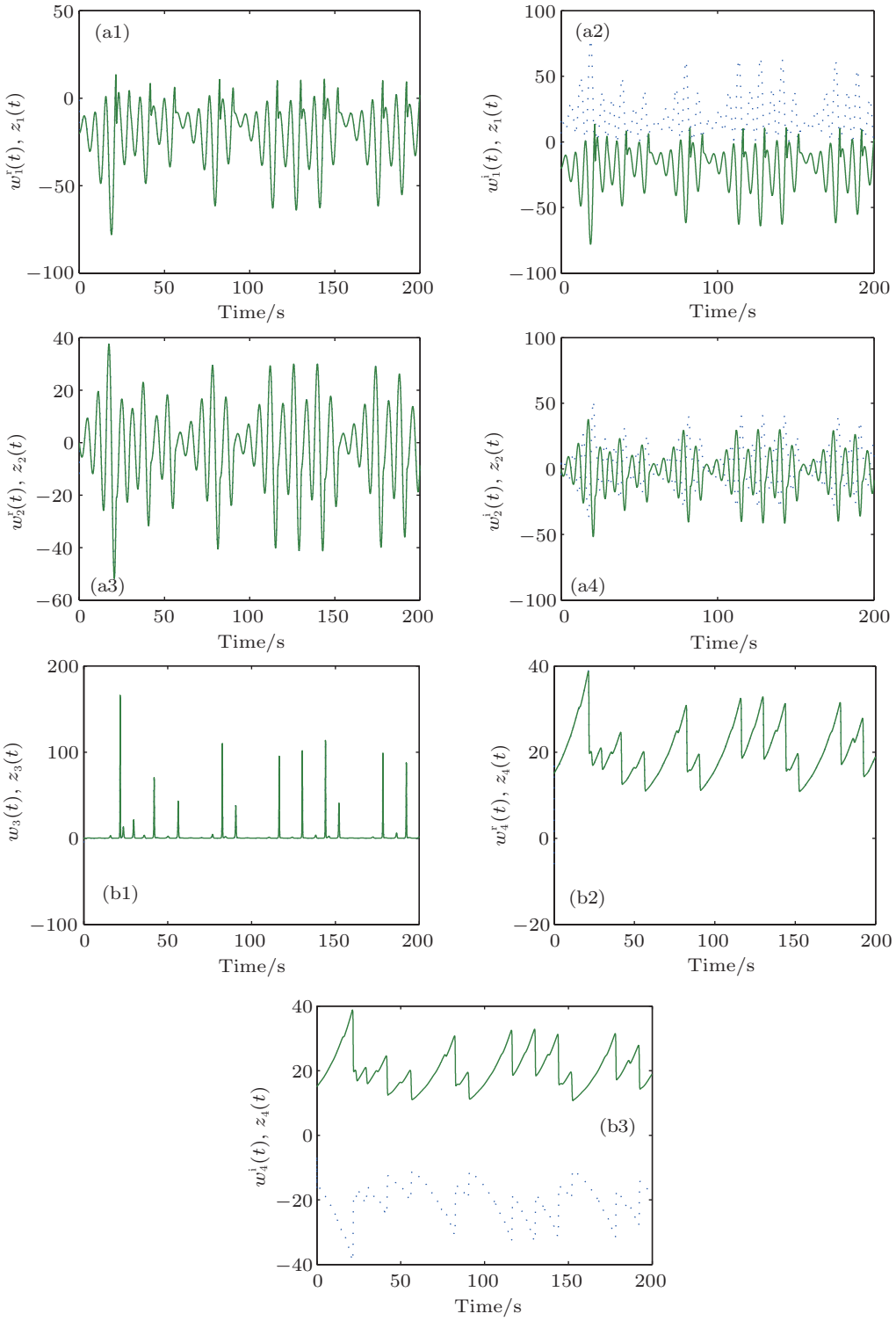


Fig. 1. (color online) The CMPS of systems (35) and (36) with $\eta_1 = 0.05$, $\eta_2 = \eta_3 = 1$, $\eta_4 = \eta_5 = 0.1$, $\lambda_1 = \lambda_2 = \lambda_3 = \lambda_4 = \lambda_5 = 0.01$, $\varsigma_1 = \varsigma_2 = \varsigma_3 = \varsigma_4 = 0.01$, $\tau_1 = 0.05$, $\tau_2 = \tau_3 = 1$, $\tau_4 = 0.1$, $\gamma_1 = \gamma_2 = \gamma_3 = \gamma_4 = 10$ and complex scaling factors $1-$ j, $1-$ j, 1, $1-$ j. Panel (a) [(a1)–(a4)]: The CMPS of state variables w_1, z_1 and w_2, z_2. Panel (b) [(b1)–(b3)]: The CMPS of state variables w_3, z_3 and w_4, z_4.

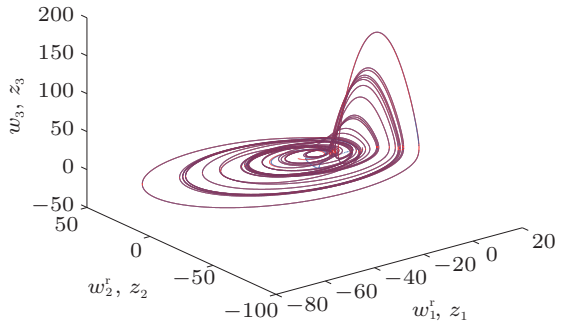


Fig. 2. (color online) The real parts $(w_1^{\mathrm{r}}, w_2^{\mathrm{r}}, w_3)$ of system (36) synchronize (z_1, z_2, z_3) of system (35) as $h_1 = h_3 = h_5 = 1$.

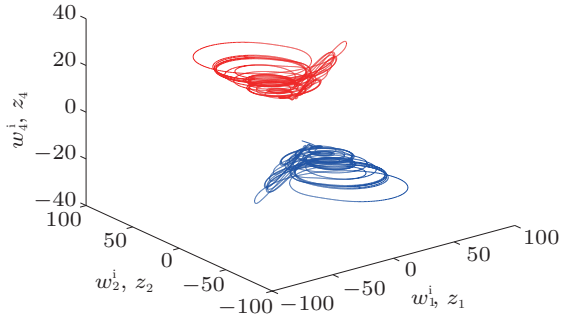


Fig. 3. (color online) The imaginary parts $(w_1^{\mathrm{i}}, w_2^{\mathrm{i}}, w_4^{\mathrm{i}})$ of system (36) anti-synchronize (z_1, z_2, z_4) of system (35) as $h_2 = h_4 = h_7 = -1$.

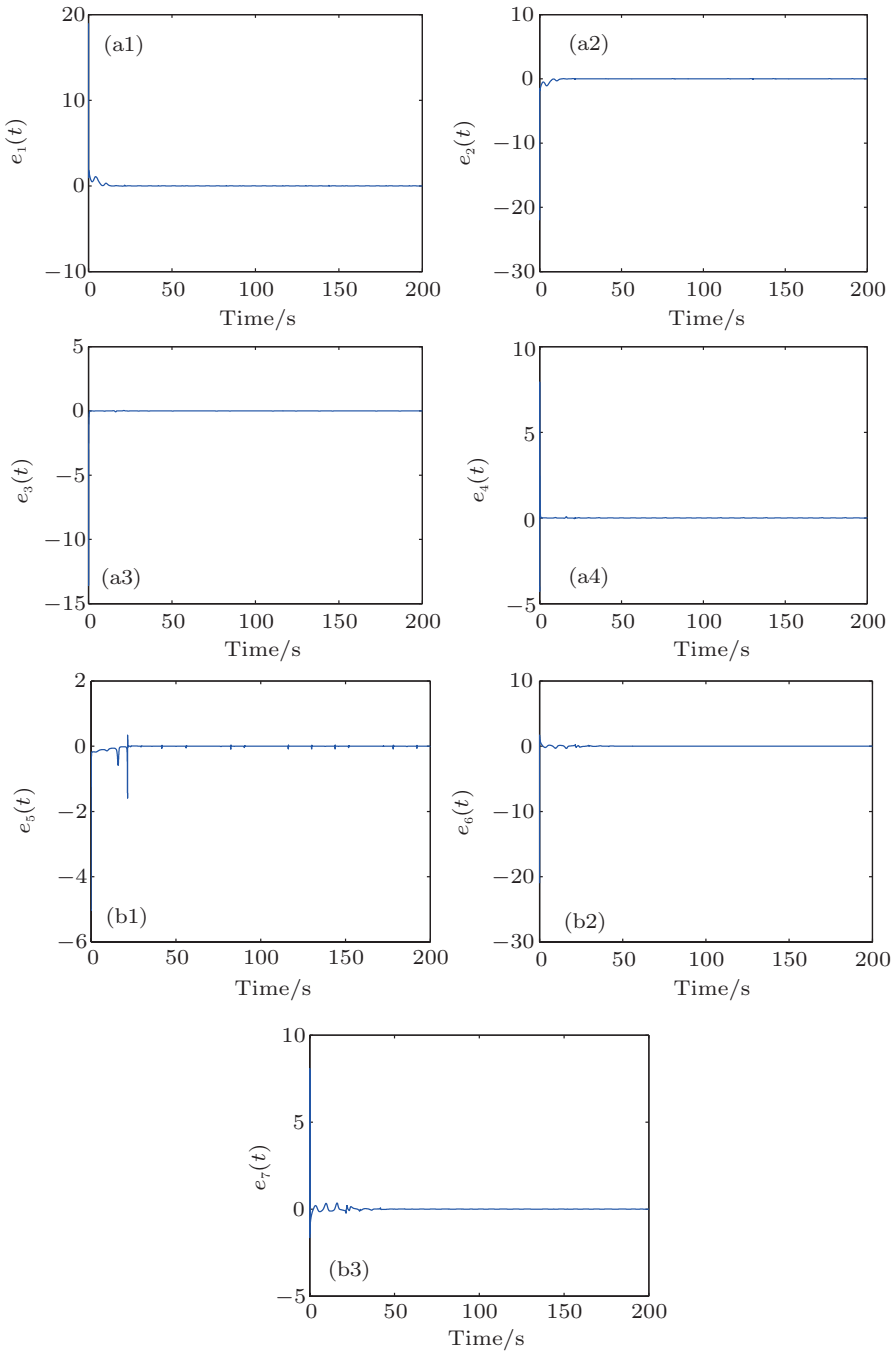


Fig. 4. (color online) The error dynamic of CMPS of systems (35) and (36). Panel (a) [(a1)–(a4)]: The error between complex state variables x_1, $(1-\mathrm{j})z_1$ and w_2, $(1-\mathrm{j})z_2$. Panel (b) [(b1)–(b3)]: The error between complex state variables x_3, z_3, and x_4, $(1-\mathrm{j})z_4$.

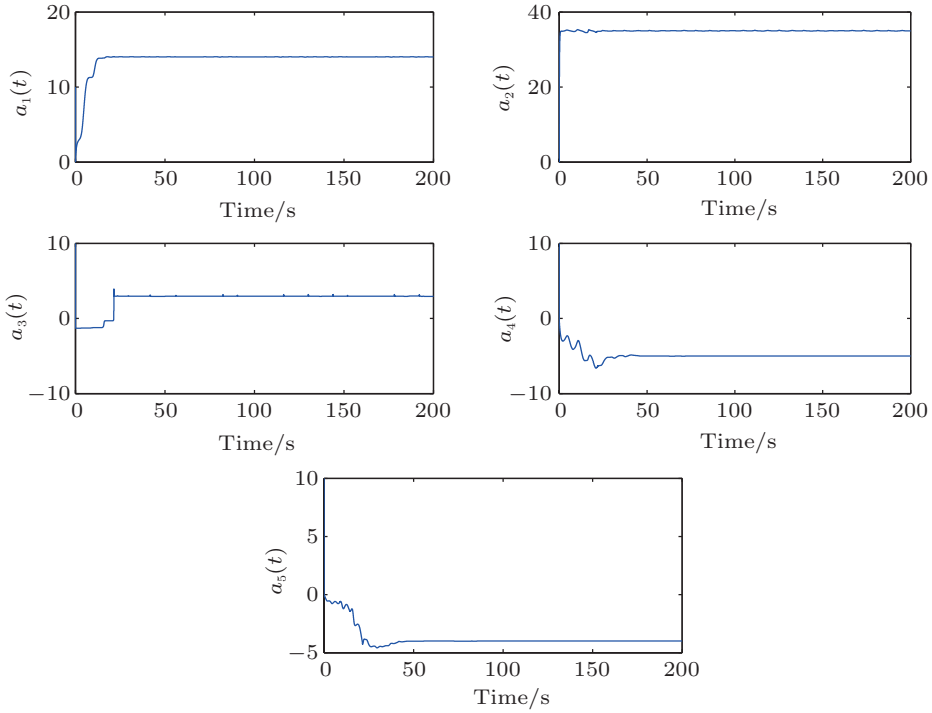


Fig. 5. (color online) The identification process of unknown parameter vector $\boldsymbol{A}$.

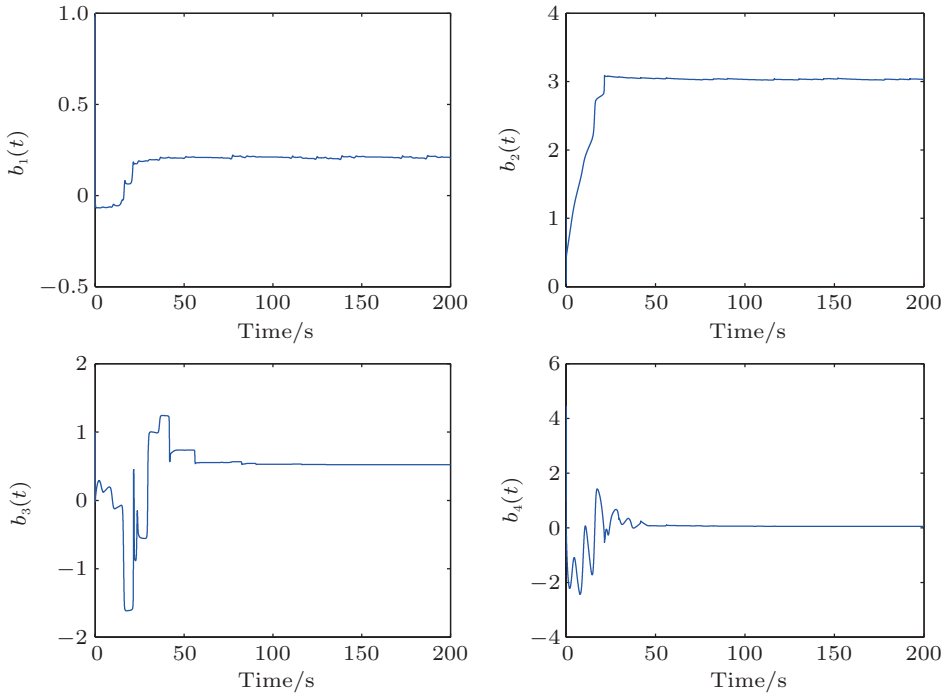


Fig. 6. (color online) The identification process of unknown parameter vector $\boldsymbol{B}$.

where

$$\boldsymbol{Q}(\boldsymbol{y}) = \begin{pmatrix} y_2 - y_1 & 0 & 0 \\ 0 & y_1 & 0 \\ 0 & 0 & -y_3 \end{pmatrix},$$

$$\boldsymbol{q}(\boldsymbol{y}) = \begin{pmatrix} 0 \\ -y_1 y_3 - y_2 \\ (1/2)(\bar{y}_1 y_2 + y_1 \bar{y}_2) \end{pmatrix},$$

and $y_1 = u_1' + \mathrm{j}u_2'$ and $y_2 = u_3' + \mathrm{j}u_4'$ are complex state variables, and $y_3 = u_5'$ is a real state variable, $\boldsymbol{D} = (d_1, d_2, d_3)^{\mathrm{T}}$ is the unknown parameter vector.

The real response Lorenz system is

$$\begin{cases} \dot{x}_1 = c_1(x_2 - x_1), \\ \dot{x}_2 = c_2 x_1 - x_2 - x_1 x_3, \\ \dot{x}_3 = -c_3 x_3 + x_1 x_2, \end{cases} \tag{42}$$

where

$$\boldsymbol{P}(\boldsymbol{x}) = \begin{pmatrix} x_2 - x_1 & 0 & 0 \\ 0 & x_1 & 0 \\ 0 & 0 & -x_3 \end{pmatrix}, \ \boldsymbol{p}(\boldsymbol{x}) = \begin{pmatrix} 0 \\ -x_2 - x_1 x_3 \\ x_1 x_2 \end{pmatrix},$$

where x_1, x_2, x_3 are real state variables, and c_1, c_2, c_3 are real unknown parameters.

We design the controller according to Theorem 3 as follows:

$$\begin{aligned} \boldsymbol{v} &= -\boldsymbol{P}(\boldsymbol{x})\hat{\boldsymbol{C}} - \boldsymbol{p}(\boldsymbol{x}) + (\boldsymbol{H}^{\mathrm{r}}\boldsymbol{Q}(\boldsymbol{y})^{\mathrm{r}} - \boldsymbol{H}^{\mathrm{i}}\boldsymbol{Q}(\boldsymbol{y})^{\mathrm{i}})\hat{\boldsymbol{D}} + \boldsymbol{H}^{\mathrm{r}}\boldsymbol{q}(\boldsymbol{y})^{\mathrm{r}} - \boldsymbol{H}\boldsymbol{q}(\boldsymbol{y})^{\mathrm{i}} + \boldsymbol{K}\boldsymbol{e} \\ &= \begin{pmatrix} -\hat{c}_1(x_2 - x_1) + [h_1(u_3' - u_1') - h_2(u_4' - u_2')]\hat{d}_1 + k_1 e_1 \\ -\hat{c}_2 x_1 + x_2 + x_1 x_3 + (h_3 u_1' - h_4 u_2')\hat{d}_2 - h_3(u_1' u_5' + u_3') + h_4(u_2' u_5' + u_4') + k_2 e_2 \\ \hat{c}_3 x_3 - x_1 x_2 + h_5(-\hat{d}_3 u_5' + u_1' u_3' + u_2' u_4') + k_3 e_3 \end{pmatrix}, \end{aligned} \tag{43}$$

where $h_1 + \mathrm{j}h_2$, $h_3 + \mathrm{j}h_4$, h_5 are scaling factors, $e_1 = x_1 - (h_1 u_1' - h_2 u_2')$, $e_2 = x_2 - (h_3 u_3' - h_4 u_4')$, and $e_3 = x_3 - h_5 u_5'$.

The adaptive laws are taken as expression (26) where

$$\nabla_{\hat{\boldsymbol{C}}}\omega(\hat{\boldsymbol{C}}, \hat{\boldsymbol{D}}, t) = \begin{pmatrix} -(x_2 - x_1)e_1 \\ -x_1 e_2 \\ x_3 e_3 \end{pmatrix}, \tag{44}$$

$$\nabla_{\hat{\boldsymbol{D}}}\omega(\hat{\boldsymbol{C}}, \hat{\boldsymbol{D}}, t) = \begin{pmatrix} e_1[h_1(u_3' - u_1') - h_2(u_4' - u_2')] \\ e_2(h_3 u_1' - h_4 u_2') \\ -u_5' e_5 \end{pmatrix}, \tag{45}$$

and

$$\dot{\boldsymbol{k}} = \begin{pmatrix} \dot{k}_1 \\ \dot{k}_2 \\ \dot{k}_3 \end{pmatrix} = \begin{pmatrix} -\gamma_1 e_1^2 \\ -\gamma_2 e_2^2 \\ -\gamma_3 e_3^2 \end{pmatrix}. \tag{46}$$

The true values of unknown parameters are $\boldsymbol{C} = (10, 28, 8/3)^{\mathrm{T}}$ and $\boldsymbol{D} = (35, 55, 8/3)^{\mathrm{T}}$. The initial conditions are $\boldsymbol{y}(\boldsymbol{0}) = (-1 - 2\mathrm{j}, -3 - 4\mathrm{j}, -5)^{\mathrm{T}}$ and $\boldsymbol{x}(\boldsymbol{0}) = (-1, -3, -5)^{\mathrm{T}}$. The initial values of estimated parameters and control strength are $\hat{\boldsymbol{C}}(0) = (20, 20, 20)^{\mathrm{T}}$, $\hat{\boldsymbol{D}}(0) = (10, 10, 10)^{\mathrm{T}}$, and $\boldsymbol{k}(0) = (0, 0, 0)^{\mathrm{T}}$. The fourth-order Runge–Kutta scheme is utilized to solve the differential equations with $\Delta t = 10^{-3}$ s. The CMPS process of systems (41) and (42) is shown in Fig. 7, where the solid line shows the states of the drive system and the dotted line presents the states of the response system. Their chaotic behaviors are shown in Fig. 8, where the red line shows the trajectory of the drive system and the blue line presents the trajectory of the response system. The response system (42) synchronizes the real parts of the product of $\boldsymbol{H}$ and complex drive system (41) in Fig. 8. The errors of CMPS converge asymptotically to zero as demonstrated in Fig. 9. The processes of parameters identification of $\hat{\boldsymbol{C}}$ and $\hat{\boldsymbol{D}}$ are shown in Fig. 10. Obviously, the estimated values of $\hat{\boldsymbol{C}}$ and $\hat{\boldsymbol{D}}$ converge to certain constants.

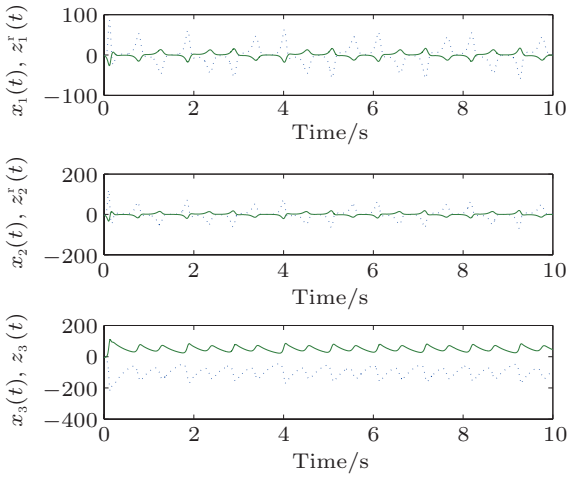


Fig. 7. (color online) The CMPS of systems (41) and (42) with $\eta_1 = \eta_2 = \eta_3 = 1$, $\lambda_1 = \lambda_2 = \lambda_3 = 0.01$, $\varsigma_1 = \varsigma_2 = \varsigma_3 = 0.01$, $\tau_1 = \tau_2 = \tau_3 = 1$, $\gamma_1 = \gamma_2 = \gamma_3 = 1$, and complex scaling factors $-2+\mathrm{j}, -2+\mathrm{j}, -2$.

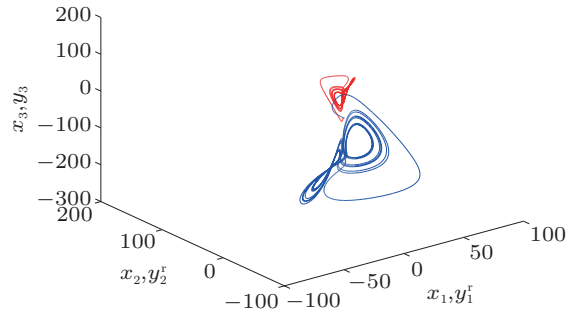


Fig. 8. (color online) The response system (42) synchronizes the real parts $(-2y_1^{\mathrm{r}} - y_1^{\mathrm{i}}, -2y_2^{\mathrm{r}} - y_2^{\mathrm{i}}, -2y_3)$ of the product that the drive system (41) multiplied by complex scaling factors $-2+$ j, $-2+$ j, -2.

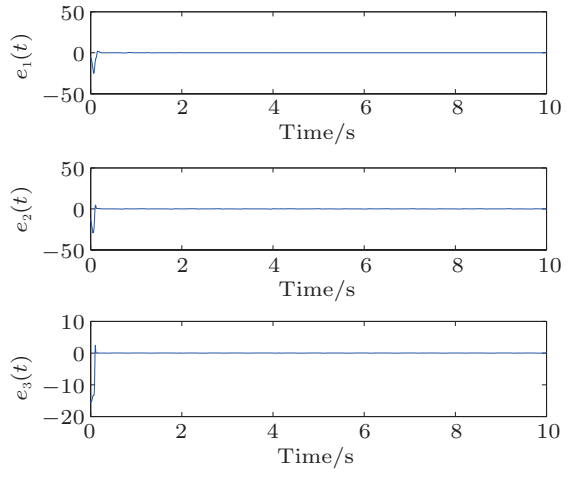


Fig. 9. (color online) The error dynamic of CMPS with $-2+$ j, $-2+$ j, -2 of systems (41) and (42). Here $e_1 = x_1 - (-2y_1^{\mathrm{r}} - y_1^{\mathrm{i}})$, $e_2 = x_2 - (-2y_2^{\mathrm{r}} - y_2^{\mathrm{i}})$, and $e_3 = x_3 - (-2y_3)$.

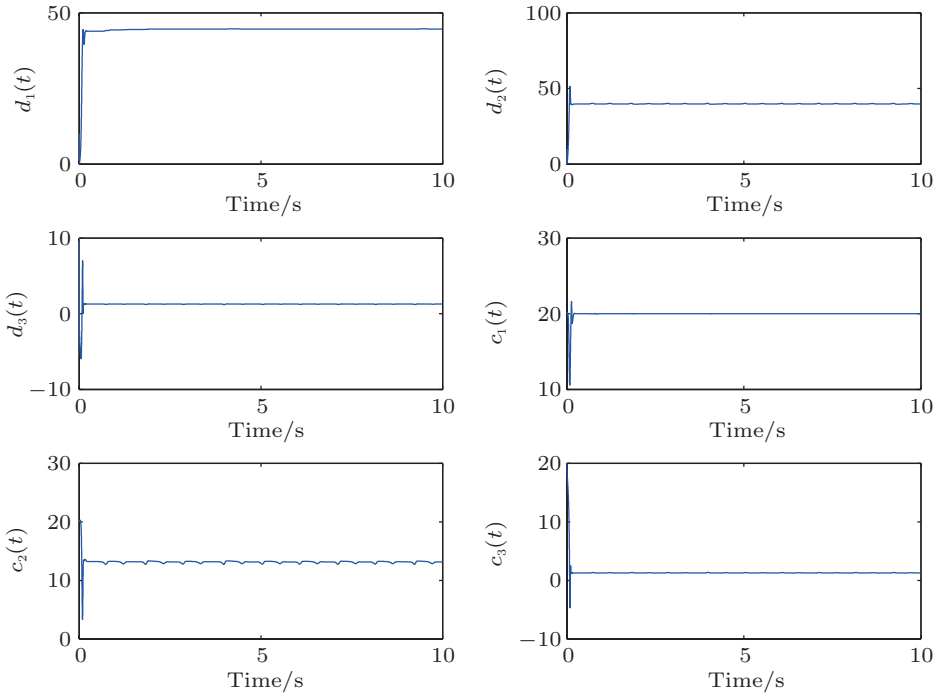


Fig. 10. (color online) The identification process of unknown parameter vectors $\boldsymbol{C}$ and $\boldsymbol{D}$.

6. Conclusion

We give the definition of CMPS of complex chaotic systems and real chaotic systems and design corresponding adaptive CMPS schemes considering all situations of unknown parameters and pseudo-gradient condition based on the SG method. The convergence factors and the dynamical control strength are added to regulate the convergence speed and increase the robustness of the uncertain response system, which is significant in practical applications. The theoretical result is verified by numerical examples, and the simulations demonstrate the effectiveness of the proposed synchronization scheme.

Moreover, the CMPS establishes a link between real chaotic systems and complex chaotic systems, which increases the complexity and scope of the synchronization and directs high security and large variety of secure communications.

References

[1] Pecora L M and Carroll T L 1990 *Phys. Rev. Lett.* **64** 821
[2] Yang D S, Liu Z W, Zhao Y and Liu Z B 2012 *Chin. Phys. B* **21** 040503
[3] Wang X Y, Zhang N, Ren X L and Zhang Y L 2011 *Chin. Phys. B* **20** 020507
[4] Wu D and Li J J 2010 *Chin. Phys. B* **19** 120505
[5] Feki M, Robert B, Gelle G and Colas M 2003 *Chaos, Solitions and Fractals* **18** 881
[6] Fowler A C and Gibbon J D 1982 *Physica D* **4** 139
[7] Mahmoud G M and Bountis T 2004 *Int. J. Bifur. Chaos* **14** 3821
[8] Mahmoud G M, Bountis T and Mahmoud E E 2007 *Int. J. Bifur. Chaos* **17** 4295
[9] Li Z G and Xu D L 2004 *Chaos, Solitions and Fractals* **22** 477
[10] Mahmoud G M and Mahmoud E E 2010 *Nonlinear Dyn.* **61** 141
[11] Mahmoud G M and Mahmoud E E 2010 *Nonlinear Dyn.* **62** 875
[12] Liu S T and Liu P 2011 *Nonlinear Anal.-Real* **12** 3046
[13] Liu P and Liu S T 2011 *Phys. Scr.* **83** 065006
[14] Mahmoud G M and Mahmoud E E 2012 *Nonlinear Dyn.* **67** 1613
[15] Liu P, Liu S T and Li X 2012 *Phys. Scr.* **85** 035005
[16] Hu M, Yang Y Q, Xu Z Y and Guo L X 2008 *Math. Comput. Simul.* **79** 449
[17] Mahmoud G M and Mahmoud E E 2010 *Math. Comput. Simul.* **80** 2286
[18] Liu P and Liu S 2012 *Nonlinear Dyn.* **70** 585
[19] Hu M, Xu Z and Zhang R 2008 *Commun. Nonlinear Sci. Numer. Simul.* **13** 456
[20] Hu M, Xu Z and Zhang R 2008 *Commun. Nonlinear Sci. Numer. Simul.* **13** 782
[21] Chee C Y and Xu D 2005 *Chaos, Solitions and Fractals* **23** 1063
[22] Fradkov A L and Pogromsky A Y 1996 *IEEE Trans. Circ. Syst. I* **43** 907
[23] Li N, Li J F and Liu Y P 2011 *Acta Phys. Sin.* **60** 050507 (in Chinese)
[24] Zhao L D, Hu J B and Liu X H 2010 *Acta Phys. Sin.* **59** 2305 (in Chinese)
[25] Hu J B, Han Y and Zhao L D 2009 *Acta Phys. Sin.* **58** 1441 (in Chinese)
[26] Huang D 2005 *Phys. Rev. E* **71** 037203
[27] Chen S H, Hua J, Wang C P and Lü J H 2004 *Phys. Lett. A* **321** 50
[28] Mahmoud E E 2005 *Math. Comput. Model.* **55** 1951